Dynamic Simulation and Experimental Evaluation of EPDM Terpolymerization with Vanadium-Based Catalyst

MÔNICA CARCUCHINSKI HAAG,[1] JOÃO HENRIQUE ZIMNOCH DOS SANTOS,[1] JAIRTON DUPONT,[1] ARGIMIRO RESENDE SECCHI[2]

[1] Instituto de Química, Universidade Federal do Rio Grande do Sul Av. Bento Gonçalves, 9500, 91540-000, Porto Alegre, RS Brazil

[2] Depto. de Engenharia Química, Universidade Federal do Rio Grande do Sul Rua Luiz Englert, s/n 90040-040, Porto Alegre, RS Brazil

Received 7 December 1997; accepted 18 July 1998

ABSTRACT: The development of a simplified kinetic model describing some effects observed in catalyzed olefin terpolymerization is presented. Based on the method of moments, the model describes the influence of *Al/V* ratio and diene concentration on reaction yield and on polymer characteristics such as molecular weight, ethylene incorporation, and polydispersity. In order to verify the model validity, the terpolymerization reactions were performed using $VOCl_3$–$Al_2Et_3Cl_3$ systems and 2-ethylidenebicyclo[2.2.1]hept-5-ene (ENB) as diene. The results of dynamic simulation fit well the experimental data for *Al/V* up to 15, but the model fails under high diene concentration, where branching reactions, neglected by reason of simplification, become significant.
 J Appl Polym Sci 70: 1173–1189, 1998

Key words: vanadium catalysts; modeling; olefin terpolymerization; EPDM

INTRODUCTION

The intrinsic complexity of ethylene–propylene–diene (EPDM) terpolymerization with Ziegler–Natta catalysts demands reaction models in order to control and to better understand the polymerization process.

Ziegler–Natta systems are among the most studied in modeling.[1–4] However, a few complete models for ethylene–propylene (EP) copolymerization or (ethylene–propylene–diene–methylene) EPDM terpolymerization, employing vanadium-based catalyst, were published in the literature. Valvassori et al.[5] performed one of the first systematic kinetic studies of ethylene–propylene copolymerization, employing VCl_4–$Al(Hex)_3$ systems. Podolnyi et al.[6] studied the effect of 2-ethylidenebi-cyclo[2.2.1]hept-5-ene (ENB) in ethylene and propylene copolymerization kinetic constants in the presence of $VOCl_3$–$Al_2Et_3Cl_3$, employing a batch system under monomer constant pressure. He assumed all reactions as instantaneous and observed a higher ethylene reactivity with the diene introduction. Moreover, he realized that ENB reactivity is higher in a growing chain terminated with ethylene than with propylene.

Cozewith[7] built a more complex kinetic model of the terpolymerization reaction with vanadium salt–alkylaluminum catalyst components, based on pilot plant studies in a continuously-stirred tank reactor (CSTR). In that proposed kinetic model, he considered catalyst activation and deactivation, chain initiation with ethylene, chain propagation, spontaneous chain termination, chain termination by diene and propylene, and transfer reaction with propylene, hydrogen, and alkylaluminum. Cozewith verified the influence of

Correspondence to: J. H. Z. dos Santos (jhzds@if.ufrgs.br).
Journal of Applied Polymer Science, Vol. 70, 1173–1189 (1998)
 CCC 0021-8995/98/061173-17

the *Al/V* ratio on the molecular weight under different catalytic systems. In the case of terpolymerization with a $VOCl_2(OEt)$–$AlEt_2Cl$ catalytic system, the alkylaluminum presented a high influence on chain transfer reactions. He considered that polymeric chain lifetime was not instantaneous, as previously proposed by Podolnyi et al.[6] but it was in order of minutes.

Pronyayev et al.,[8] employing the $VOCl_3$–$Al_2Et_3Cl_3$ system and an experimental unit identical to the one used by Podolnyi,[6] studied the copolymerization kinetic taking into account chain transfer reaction with polymers, catalyst activation, and reactivation by monomers for the EP copolymerization. He concluded that the activation and deactivation rates were very similar. The number of active centers was around 15 to 40% of the initial $VOCl_3$ concentration.

Cozewith[9] also studied the influence of the hydrogen on the molecular weight for the $VOCl_3$–$Al_2Et_3Cl_3$ catalytic system on the EP copolymerization in a CSTR reactor. In order to produce monodisperses polymers, in a latter study, he modeled the EP copolymerization using a plug flow reactor (PFR). It is worth mentioning that this author observed that the compositional distribution was not homogeneous due to the ethylene-to-propylene ratio variation along the reactor since ethylene is more reactive than propylene.

Most of the models proposed in the literature did not deal with a complete approach of the terpolymerization reaction. For instance, Podolnyi and Pronyayev published simplified mathematical models aiming at the kinetic constant determination. Nevertheless, none of them presented the detailed set of equations employed in the model reaction for EPDM terpolymerization. The only models presented were based on homopolymerization reaction.

This article focuses on modeling the kinetics of vanadium-catalyzed olefin terpolymerization in a semibatch reactor, where the monomers (gas phase) are fed continuously under a constant rate, while the liquid phase is operated in batch. Such conditions guarantee a homogeneous comonomer composition and prevent the generation of more than 1 catalytic species in the reaction milieu, giving a narrow molecular weight distribution.

Our proposed model is based on an experimental system similar to the one adopted by Podolnyi, as follows: in semibatch, with continuous ethylene and propylene feeding, employing 2-ethylidenebi-cyclo[2.2.1]hept-5-ene (ENB) as the diene and $VOCl_3$–$Al_2Et_3Cl_3$ as the catalytic system. Nevertheless, this model differs from the one developed by Podolnyi on considering the terpolymerization as a dynamic process. It is worth mentioning that this selected catalytic system guarantees the existence of a unique active species.[10] The influence of the *Al/V* ratio and of diene concentration was evaluated in terms of dynamic simulation and compared to experimental data.

EXPERIMENTAL

Chemicals

Polymerization-grade ethylene and propylene were purchased from White–Martins (Porto Alegre, Brazil) and dried using molecular sieve (0.4 nm) columns. Hexane was dried by refluxing over metallic sodium, followed by distillation under argon atmosphere. 2-ethylidenebi-cyclo[2.2.1]hept-5-ene (ENB), the catalyst precursor $VOCl_3$ (0.23*M* in hexane), and the cocatalyst $Al_2Et_3Cl_3$ (1.00*M* in hexane) were donated by NITRIFLEX S.A.

Polymerization Reactions

The polymerizations were carried out in a 2-L glass reactor (Büchi) using *n*-hexane as the solvent. The diene, the vanadium compound, and the required amount of cocatalyst were introduced in this order into the reactor containing hexane (1 L) at 0°C under positive pressure of a mixture of ethylene and propylene (1 : 3 in mass, according to gas chromatography analysis of the gas phase). The temperature was then increased to 15°C under a continuous flow of ethylene and propylene for 30 min. The reaction was then quenched by the addition of ethanol (at room temperature). The polymer was collected, washed with ethanol (1 L), and vacuum-dried at 135°C for 60 min.

Polymers Characterization

The polymer films were characterized by infrared (IR) spectroscopy [Mattson 3020 Fourier transform IR (FTIR) spectrophotometer] measuring the ratio of the intensities of the 1155-cm^{-1} methyl band and the 720-cm^{-1} methylene band according to ASTM D3900. The diene incorporation was monitored by the intensity of the 817-cm^{-1} band and compared to those obtained from commercial polymer samples with known iodine numbers.

The glass transition temperature (T_g) of the polymers was determined using differential scan-

ning calorimetry (12000 PL-DSC) with a heating rate of 20°C · min^{-1}, while the average viscosity molecular weight ($\overline{M_V}$) was determined with an Ubbelohde-type viscometer using decalin as solvent at 135°C. Molecular weight and molecular weight distribution were determined by means of gel permeation chromatography (GPC, Waters 150C) in 1,2,4-trichlorobenzene at 140°C. The data were analyzed using polystyrene calibration curves.

THE KINETIC MODEL

Carrying out this investigation, it is first useful to consider the generally accepted mechanisms, which may be found throughout the literature. According to those, we arrive at a general set of equations and rate expressions presented in Table I, adapted from Cozewith.[9]

As we can see from Table I, the catalyst (C_1) must undergo activation by the alkyl cocatalyst in a rapid and complete reaction or might be deactivated by a spontaneous reaction (k_x) or by a reaction with diene (k_{x3}). In the studied system, the diene deactivation is extremely important since the monomer itself can cause the irreversible reduction of V (III) to V (II), inactive for polymerization.[11] For this reason, it was only taking into account the deactivation by ENB.

Chain growth begins with initiation step due to ethylene and propylene, as assumed previously by Cozewith.[9] Some authors consider only the role of ethylene in this reaction step.[6,7] The chain growth is followed by a rapid chain propagation, resulting from the combination of each 3 monomers, which would theoretically generate 9 equations. Nevertheless, we neglected the following combinations: diene–diene, diene–propylene, and propylene–diene, due to the extremely low diene incorporation in such copolymers, as previously proposed by Cozewith.[7]

The polymer molecular weight is controlled by chain transfer with agents, like hydrogen (not considered in our model) or alkyl cocatalyst, creating a dead polymer chain (U_i) and a vacant active site. Chain transfer may also occur due to reaction with propylene; in this case, such reaction leads to the formation of a live polymer unitary chain (Q_1).

Finally, the mechanisms of site deactivation may occur spontaneously (k_t) or with the monomer, propylene (k_{tm2}), or diene (k_{tm3}). In both cases, those reactions create permanently deactivated sites (D), and the growing polymer chain is terminated (U_i or U_{i+1}).

The standard Ziegler–Natta scheme does not account for branching reactions, which proceed from the reaction of chain branches via internal and terminal double bond polymerization. The unreacted double bonds on dead polymer species can be produced by the introduction of a diene (as in the present system) or by the inherent nature of chain transfer mechanisms. In other words, polymers formed with dienes will possess unreacted double bonds hanging off the chain, which then can eventually react at an active site to form a tetrafunctional branch point via the internal double bond branching reaction. The unsaturation that results from the latter chain transfer mechanism can react similarly to generate a trifunctional branch point via the terminal double bond branching reaction. Very recently, a long chain branching modeling was discussed in the literature.[12] In our system, taking into account the low branching reaction rate for ENB, those reactions were not added to the model.

Most reactions in Table I present a bimolecular kinetics, except the ones concerning the catalyst activation, deactivation, and chain spontaneous termination. According to Cozewith,[9] the best correlation for the transfer reaction rate with alkylaluminum is obtained by replacing the aluminum concentration by the ratio of alkylaluminum–ethyl bonds to vanadium, which are calculated by assuming that vanadium catalyst is reduced to a valence of 3 during catalyst activation and that 1 alkyl group reduces 1 vanadium by 1 valence unit.

MATHEMATICAL MODEL

The equations that compose the mathematical model, based on mass and energy balance, were done after the polymerization unit represented in Scheme 1. The monomers (ethylene and propylene) were continuously introduced in a 2-L glass vessel, solubilized in the liquid phase, being finally removed by an on–off control pressure regulator. Gas feed flow rates were measured and controlled with Brooks flowmeters previously calibrated. The use of continuous gas flow aimed to maintain constant the relative monomeric composition in the liquid phase, as well as the terpolymer composition. If a batch system were employed, we would have a propylene-enriched gas phase due to the higher activity of ethylene.

Table I General Kinetic Scheme for Catalyzed Olefin Terpolymerization Kinetic Model

Reaction		CTE	Reaction
Activation		k_a	$C_1 \xrightarrow{k_a} C_2$
Deactivation	Poison	k_x	$C_1 \xrightarrow{k_x} D$
	Diene	k_{x3}	$C_1 + M_3 \xrightarrow{k_{x3}} D$
Chain initiation	Ethylene	k_{y1}	$C_2 + M_1 \xrightarrow{k_{y1}} P_1$
	Propylene	k_{y2}	$C_2 + M_2 \xrightarrow{k_{y2}} Q_1$
Chain propagation	Ethylene	k_{11}	$P_i + M_1 \xrightarrow{k_{11}} P_{i+1}$
		k_{12}	$P_i + M_2 \xrightarrow{k_{12}} Q_{i+1}$
		k_{13}	$P_i + M_3 \xrightarrow{k_{13}} R_{i+1}$
	Propylene	k_{21}	$Q_i + M_1 \xrightarrow{k_{21}} P_{i+1}$
		k_{22}	$Q_i + M_2 \xrightarrow{k_{22}} Q_{i+1}$
		k_{23}	$Q_i + M_3 \xrightarrow{k_{23}} R_{i+1}$
	Diene	k_{31}	$R_i + M_1 \xrightarrow{k_{31}} P_{i+1}$
		k_{32}	$R_i + M_2 \xrightarrow{k_{32}} Q_{i+1}$
Chain transfer	Propylene	k_{trm2}	$P_i + M_2 \xrightarrow{k_{trm2}} U_i + Q_1$
	Al-alkyl	k_{tr2}	$P_i + Al \xrightarrow{k_{tr2}} U_i + P_1$
Chain termination	Deactivation	k_t	$P_i \xrightarrow{k_t} U_i + D$
	Propylene	k_{tm2}	$P_i + M_2 \xrightarrow{k_{tm2}} U_{i+1} + D$
	Diene	k_{tm3}	$P_i + M_3 \xrightarrow{k_{tm3}} U_{i+1} + D$

CTE: kinetic constant

The solvent (Hexane, Hx), the cocatalyst (Al), the catalyst ($VOCl_3$), and the diene (ENB) were added in batch and assumed that they were homogeneously dispersed in the liquid phase.

The reactor temperature was indirectly regulated by a proportional controller in the temperature of the ethylic alcohol bath. The reactor pressure was maintained through an on–off control valve placed at the outlet of the reactor. If the internal pressure (P_T) was higher than the set point pressure, the valve released the exceeding pressure.

The instantaneous data, such as temperature, pressure, and stirring rate, were recorded using a Büchi Data System (BDS-388). After a predefined polymerization time, the reaction was then terminated by shutting off the feed streams, followed

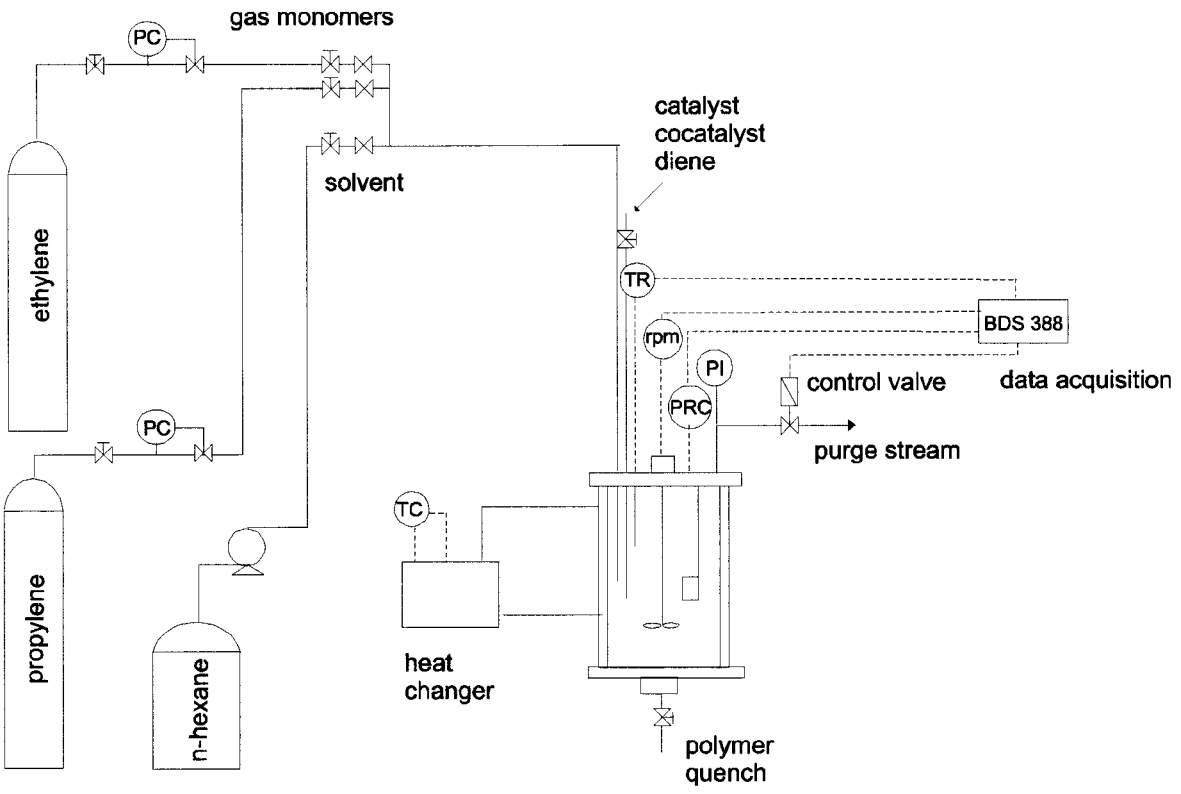

Scheme 1

by nitrogen purge and precipitating the polymer in ethanol.

Our model was not based on the assumption of a quasi-steady-state condition. According to this assumption, the polymeric chain building is practically instantaneously, and the following simplification concerning the live chains (P) in the milieu could be adopted:

$$\frac{dP}{dt} \cong 0 \tag{1}$$

Cozewith[7] pointed out that this chain building time is of the order of 1 to 3 min. Thus, in our model, we did not perform the above-mentioned simplification and opted for the dynamic study of the terpolymerization reaction.

The liquid and the gas phase volumes were assumed constant during polymerization. According to this assumption, there is no variation in volume regarding the mass balance.

Moreover, it is also worth mentioning that only the monomer present in the liquid phase is capable of participating in the polymerization since the reaction takes place only in that phase. Thus, taking into account the above-mentioned considerations, the mass balance can be done separately in the liquid and in the gas phase. In the following description, the indexes G and L will be related, respectively, to gas and to liquid phase. For instance, M_{ETG} means the ethylene monomer in the gas phase.

Mass Balance in the Gas Phase

The mass balance in the gas phase was performed for each gas (ethylene and propylene) and for the solvent due to its vapor pressure.

The mass balance for ethylene present in gas phase (M_{ETG}) is obtained taking into account the gas flow into and out of the reactor, and the mass transferred by convection to liquid phase.

According to Floyd et al.,[13] the transfer rate by convection per volume unit (R_{OB}) is calculated through equation (2).

$$R_{OB} = kla(M_{\mathrm{EQ}} - M) \tag{2}$$

where M_{EQ} is the monomer concentration in equilibrium, M is the instantaneous monomer concentration, and kla is the overall mass transfer coefficient based on the liquid phase. This coefficient is in

fact the combination of mass transfer coefficient kl[14] with the interfacial specific area a.[15] In view of the difficulty to determine experimentally these parameters, we estimated them from data published by Floyd et al. for propylene homopolymerization[13] correlating parameters such as stirring rate, reactor volume, and temperature with those used in our system. In our model, we assumed that for the lab-scale reactor, the mass transfer resistance for ethylene and propylene were of the same magnitude, based on the experimental conditions such as homogeneous reaction, high stirring rates, and high monomer concentration.

The ethylene accumulation in the gas phase (M_{ETG}) is obtained by equation (3), where M_{ETF} represents the amount that is introduced into the system, and M_{ETGS} is the amount released by the pressure control valve. Similarly, equation (4) represents the same balance in the case of propylene.

$$\frac{dM_{\mathrm{ETG}}}{dt} = \frac{F_{\mathrm{ET}}}{V_G} M_{\mathrm{ETF}} - kla_{\mathrm{ET}} \frac{V_L}{V_G} (M_{\mathrm{ETEQ}} - M_{\mathrm{ETL}}) - \frac{F_G}{V_G} M_{\mathrm{ETGS}} \quad (3)$$

$$\frac{dM_{\mathrm{PPG}}}{dt} = \frac{F_{\mathrm{PP}}}{V_G} M_{\mathrm{PPF}} - kla_{\mathrm{PP}} \frac{V_L}{V_G} (M_{\mathrm{PPEQ}} - M_{\mathrm{PPL}}) - \frac{F_G}{V_G} M_{\mathrm{PPGS}} \quad (4)$$

Mass Balance in the Liquid Phase

The mass balance concerning the liquid phase took into account the presence of catalyst, cocatalyst, monomers, live and dead polymeric chains, and the solvent itself.

The concentration of deactivated catalyst (D) is due to poisoning, vanadium oxide formation, and deactivation by vanadium itself present in the reaction milieu [eq. (5)].

$$\frac{dD}{dt} = (\mathrm{k_x} + \mathrm{k_{x3}} M_{\mathrm{DI}}) C_1 \quad (5)$$

The concentration of nonactivated catalyst (C_1) decreases due to the above-mentioned reactions, besides the active species (C_2) generation reaction, as follows:

$$\frac{dC_1}{dt} = -(\mathrm{k_x} + \mathrm{k_{x3}} M_{\mathrm{DI}} + \mathrm{k_a}) \mathrm{C_1} \quad (6)$$

The activated species (C_2) are formed by activation and chain transfer reactions but consumed by the initiation reaction, including both monomers, ethylene (P_1) and propylene (Q_1):

$$\frac{dC_2}{dt} = \mathrm{k_a} C_1 - \mathrm{k_{y1}} C_2 M_{\mathrm{ETL}} - \mathrm{k_{y2}} C_2 M_{\mathrm{PPL}} + \left[\mathrm{k_{trm2}} M_{\mathrm{PPL}} + \mathrm{k_{tr2}} \left(\frac{Al_0}{C_{10}} - 1 \right) \right] (P_1 + Q_1) \quad (7)$$

In the above expression, the transfer reactions to the activated monomers (P_1 and Q_1) are proportional to initial cocatalyst-to-catalyst ratio (Al_0/C_{10}) following the expression proposed by Cozewith[9] for this catalytic system. For higher diene concentration, the initial vanadium concentration (C_{10}) was corrected taking account the reduction to V(II) by the diene. In that way, the initial alkylaluminum concentration (Al) is reduced by transfer reactions that are proportional to initial cocatalyst/catalyst ratio (Al_0/C_{10}):

$$\frac{dAl}{dt} = -\mathrm{k_{tr2}} \left(\frac{Al_0}{C_{10}} - 1 \right) (P^0 + Q^0 + R^0) \quad (8)$$

To express the monomers' concentrations in the liquid phase, we must take into account their transfer from the gas phase by convection, discounted by the monomer consumption due to initiation and propagation reactions, considering all the live polymeric chains, which are terminated in ethylene (P^0), propylene (Q^0), and diene (R^0). In the case of the diene, its concentration only depends on catalyst deactivation, propagation, and termination reactions, as follows.

$$\frac{dM_{\mathrm{ETL}}}{dt} = kla_{\mathrm{ET}} (M_{\mathrm{ETEQ}} - M_{\mathrm{ETL}}) - (\mathrm{k_{y1}} C_2 - \mathrm{k_{11}} P^0 + \mathrm{k_{21}} Q^0 + \mathrm{k_{31}} R^0) M_{\mathrm{ETL}} \quad (9)$$

$$\frac{dM_{\mathrm{PPL}}}{dt} = kla_{\mathrm{PP}} (M_{\mathrm{PPEQ}} - M_{\mathrm{PPL}}) - (\mathrm{k_{y2}} C_2 - \mathrm{k_{12}} P^0 + \mathrm{k_{22}} Q^0 + \mathrm{k_{32}} R^0 + (\mathrm{k_{trm2}} + \mathrm{k_{tr2}})(P^0 + Q^0 + R^0)) M_{\mathrm{PPL}} \quad (10)$$

$$\frac{M_{\mathrm{DI}}}{dt} = -M_{\mathrm{DI}} (\mathrm{k_{13}} P^0 + \mathrm{k_{23}} Q^0 + \mathrm{k_{x3}} C_1 + \mathrm{k_{tm3}} (P^0 + Q^0 + R^0)) \quad (11)$$

In the case of copolymerization, 2 indexes are necessary to define the polymerization degree.

For instance, for a live polymer species $P_{n,m}$, n represents the number of ethylene units, and m, represents the number of propylene units, incorporated in the polymeric chain. Ray et al.[16] deduced the polymer weight distribution through generating functions, based upon the quasi-steady-state approach (QSSA) and the long chain hypothesis. As we cannot apply the QSSA to our system, we opted to use, for simplification reasons, a single index i, which represents a theoretical monomer, with the molecular weight being the weighed mean between the 3 monomers' molecular weight with their incorporation rate in the polymeric chain. By applying this assumption, the molecular weights and polydispersity can be deduced in analogy to the homopolymerization, which simplifies the model. It is worth mentioning that this approach might lead to a reduced error since ethylene and propylene have similar molecular weights and ENB, although much heavier, has a very low incorporation rate in the polymeric chain.

In order to evaluate the live polymer chain concentration in the reaction milieu, we applied the method of moments to the kinetic reactions to obtain a system of differential equations, which may be numerically integrated. Some mathematical relationships are required to define the live polymer moments and to provide a means of transforming the individual kinetic reactions into moment balance equations. The moments determination will permit us to calculate the number- and weight-average molecular weight, as well as the polymer polydispersity.

The polymer moment of kth order is defined according to equation (12), as follows:

$$S^k = \sum_{i=1}^{\infty} i^k S_i \tag{12}$$

Thus, the terpolymer chains with i polymerization degree (S_i) will be constituted of polymeric chains terminated in ethylene (P_i), propylene (Q_i), and diene (R_i), besides the dead polymer chains (U_i).

$$S_i = P_i + Q_i + R_i + U_i \tag{13}$$

The total zeroth-order moment is given in equation (14), as follows:

$$S^0 = \sum_{i=1}^{\infty} P_i + Q_i + R_i + U_i = \sum_{i=1}^{\infty} P_i + \sum_{i=1}^{\infty} Q_i + \sum_{i=1}^{\infty} R_i + \sum_{i=1}^{\infty} U_i \tag{14}$$

where

$$P^0 = \sum_{i=1}^{\infty} P_i \tag{15}$$

$$Q^0 = \sum_{i=1}^{\infty} Q_i \tag{16}$$

$$R^0 = \sum_{i=1}^{\infty} R_i \tag{17}$$

and

$$U^0 = \sum_{i=1}^{\infty} U_i \tag{18}$$

Applying the live polymer moment definition in the polymer chain balance and using some mathematical assumptions,[17] we were capable to determine the live polymeric chain terminated in ethylene, as shown in equation (19), as follows:

$$\frac{dP^0}{dt} = \mathrm{k_{y1}} C_2 M_{\mathrm{ETL}} + \mathrm{k_{tr2}}\left(\frac{Al_0}{C_{10}} - 1\right)(P^0 + Q^0 + R^0) + \mathrm{k_{21}} M_{\mathrm{ETL}} Q^0 + \mathrm{k_{31}} M_{\mathrm{ETL}} R^0 - P^0 \alpha \tag{19}$$

where

$$\alpha = \left(\mathrm{k_{tr2}}\left(\frac{Al_0}{C_{10}} - 1\right) + \mathrm{k_t} + (\mathrm{k_{tm2}} + \mathrm{k_{trm2}} + \mathrm{k_{12}}) M_{\mathrm{PPL}} + (\mathrm{k_{13}} + \mathrm{k_{tm3}}) M_{\mathrm{DI}}\right) \tag{20}$$

In the same way, the concentrations of live polymeric chains terminated with propylene (Q^0) and diene (R^0) are determined by

$$\frac{dQ^0}{dt} = \mathrm{k_{y2}} C_2 M_{\mathrm{PPL}} + \mathrm{k_{trm2}} M_{\mathrm{PPL}}(P^0 + Q^0 + R^0) + \mathrm{k_{12}} M_{\mathrm{PPL}} P^0 + \mathrm{k_{32}} M_{\mathrm{PPL}} R^0 - \beta Q^0 \tag{21}$$

where

$$\beta = \left(k_{tr2}\left(\frac{Al_0}{C_{10}} - 1\right) + k_t + (k_{tm2} + k_{trm2})M_{PPL} + k_{21}M_{ETL} + (k_{23}+k_{tm3})M_{DI}\right) \quad (22)$$

$$\frac{dR^0}{dt} = k_{13}P^0M_{DI} + k_{23}Q^0M_{DI} - R^0\gamma \quad (23)$$

where

$$\gamma = \left(k_{tr2}\left(\frac{Al_0}{C_{10}} - 1\right) + k_t + (k_{tm2} + k_{trm2} + k_{32})M_{PPL} + k_{31}M_{ETL} + k_{tm3}M_{DI}\right) \quad (24)$$

Finally, the concentration of dead polymeric chains in the reactor (U^0) are obtained from the transfer and termination reactions, which occur with all live polymeric chains (P^0, Q^0, and R^0).

$$\frac{dU^0}{dt} = (P^0 + Q^0 + R^0)\eta \quad (25)$$

where

$$\eta = \left(k_{tr2}\left(\frac{Al_0}{C_{10}} - 1\right) + k_t + k_{tm3}M_{DI} + (k_{tm2} + k_{trm2})M_{PPL}\right) \quad (26)$$

The higher-order moments for all live and dead polymeric chains are summarized in Table II.

With the moments S^0, S^1, and S^2, we can calculate the number-average and weight-average molecular weight ($\overline{M_N}$ and $\overline{M_W}$) and the polydispersity (DP).

$$\overline{M_N} = w\,\frac{S^1}{S^0} \quad (27)$$

where w is the hypothetical monomer molecular weight resulting from the combination of ethylene, propylene, and diene molecular weights, weighted by their cumulative molar fractions (xp_{ET}, xp_{PP}, and xp_{ENB}):

$$w = xp_{ET}\bar{M}_{ET} + xp_{PP}\bar{M}_{PP} + xp_{ENB}\bar{M}_{ENB} \quad (28)$$

The cumulative molar fractions are calculated by time integration of the rate of monomer incorporation in the polymeric chains.

The average molecular weight is calculated according to equation (29), as follows:

$$\overline{M_W} = w\,\frac{S^2}{S^1} \quad (29)$$

The polydispersity is

$$DP = \frac{\overline{M_W}}{\overline{M_N}} = \frac{S^0S^2}{(S^1)^2} \quad (30)$$

Finally, the polymer concentration (Y_P) in the reaction milieu, can be obtained by the following equation:

$$Y_P = S^0\overline{M_N} \quad (31)$$

Energy Balance

The energy balances were made for the reactor, the jacket, and the heat exchanger, assuming a perfect mixture and neglecting any enthalpy variation with the pressure.

For the reactor, we have

$$\frac{dT}{dt} = \frac{(-\Delta\overline{H_P})}{\rho_L Cp_L}R_P - \frac{U_G A_M(T - T_C)}{V_L\rho_L Cp_L} \quad (32)$$

where R_P is the total rate of propagation reactions with the 3 monomers.

The heat of polymerization ($-\Delta H_P$) was obtained by dynamic estimation using the SPEEDUP software from the experimental temperatures and polymer properties. The estimated result presents the same magnitude of that used by Hutchinson et al.[18] for modeling propylene polymerization using classical Ziegler–Natta systems.

Regarding the jacket, we previously investigated the heat transfer to the environment and observed that is negligible. Thus, for the jacket we have the following equation:

$$\frac{dT_C}{dt} = \frac{U_G A_M(T - T_C)}{\rho_R V_C Cp_R} + \frac{F_R}{V_C}(T_B - T_C) \quad (33)$$

Finally, the energy balance concerning the heat exchanger is described by equation (34), as follows:

Table II Moment Balances for Live and Dead Chains of the Generic Kinetic Scheme

Moment Balances		Equations
First order	Ethylene	$\frac{dP^1}{dt} = k_{y1}C_2M_{ETL} + k_{tr2}\left(\frac{Al_0}{C_{10}} - 1\right)(P^0 + Q^0 + R^0) + k_{11}M_{ETL}P^0 + k_{21}M_{ETL}(Q^1 + Q^0) + k_{31}M_{ETL}(R^1 + R^0) - \alpha P^1$
	Propylene	$\frac{dQ^1}{dt} = k_{y2}C_2M_{PPL} + k_{trM2}M_{PPL}(P^0 + Q^0 + R^0) + k_{22}M_{PPL}Q^0 + k_{12}M_{PPL}(P^1 + P^0) + k_{32}M_{PPL}(R^1 + R^0) - \beta Q^1$
	Diene	$\frac{dR^1}{dt} = k_{13}M_{DI}(P^1 + P^0) + k_{23}M_{DI}(Q^1 + Q^0) - \gamma R^1$
	Dead chains	$\frac{dU^1}{dt} = \left[(P^1 + P^0 + Q^1 + Q^0 + R^1 + R^0)(k_{tm2}M_{PPL} + k_{tm3}M_{DI}) + (P^1 + Q^1 + R^1)\left(k_{tr2}\left(\frac{Al_0}{C_{10}} - 1\right) + k_t + k_{trm2}\right)\right]$
Second order	Ethylene	$\frac{dP^2}{dt} = k_{y1}C_2M_{ETL} - k_{tr2}\left(\frac{Al_0}{C_{10}} - 1\right)(P^0 + Q^0 + R^0) + k_{11}M_{ETL}(2P^1 + P^0) + k_{21}M_{ETL}(Q^2 + 2Q^1 + Q^0) + k_{31}M_{ETL}(R^2 + 2R^1 + R^0) - \alpha P^2$
	Propylene	$\frac{dQ^2}{dt} = k_{y2}C_2M_{PPL} + k_{trm2}M_{PPL}(P^0 + Q^0 + R^0) + k_{22}M_{PPL}(2Q^1 + Q^0) + k_{12}M_{PPL}P^2 + k_{32}M_{PPL}R^2 - \beta Q^2$
	Diene	$\frac{dR^2}{dt} = k_{13}M_{DI}(P^2 + 2P^1 + P^0) + k_{23}M_{DI}(Q^2 + 2Q^1 + Q^0) - \gamma R^2$
	Dead chains	$\frac{dU^2}{dt} = \left((P^2 + 2P^1 + P^0 + Q^2 + 2Q^1 + Q^0 + R^2 + 2R^1 + R^0)(k_{tm2}M_{PPL} + k_{tm3}M_{DI}) + (P^2 + Q^2 + R^2)\left(k_{tr2}\left(\frac{Al_0}{C_{10}} - 1\right) + k_t + k_{trm2}\right)\right)$

$$\frac{dT_B}{dt} = \frac{F_R}{V_B}(T_C - T_B) - \frac{K_c}{V_B C p_R \rho_R}(T_B - T_{SET}) \tag{34}$$

The values of the heat transfer constant (K_c) and of the overall heat transfer coefficient (U_G) were dynamically estimated under the same experimental conditions, but without polymerization reaction, using the SPEEDUP software. We can see, in Figure 1, the experimental and the simulated temperatures of the reactor (T) and of the heat exchanger (T_B) using these estimated parameters.

To represent the on–off pressure control, the following equations were added to the model:

$$\text{if } P_T \le P_{SET}, \text{ then } F_G = 0 \tag{35}$$

$$\text{if } P_T \ge P_{SET}, \text{ then } F_G = K_G\sqrt{\frac{P_T - P_{ATM}}{\rho_G}} \tag{36}$$

Finally, to complete the model, we had to add the equations concerning the physical properties of the components. We considered an ideal gas phase due to the low-pressure system. The mono-

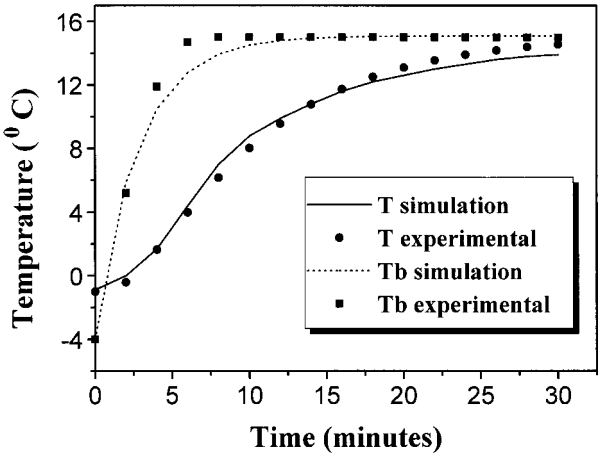

Figure 1 Temperature profiles for the reactor (—) and for heat exchanger (- -) using the estimated parameters and compared to the experimental data. [diene] = 1.8×10^{-3} mol L^{-1}; $Al/V = 8.3$.

mer equilibrium concentrations were obtained by data published by Wilhelm and Battino[19] and Floyd et al.,[13] while the flow constant (K_G) was determined experimentally.

Constant Estimation

With the proposed model, the terpolymerization reaction was simulated taking into account, initially, the polymerization constants proposed in the literature. The equations were integrated by the third-order semiimplicit Runge–Kutta method using the STIFF3 routine.[20] The initial conditions and some parameters used in the simulations are presented in Table III.

Table IV shows the kinetic constants from the literature and the ones estimated in our model. Initially, we estimated the constants by trial and error method, considering the kinetic model proposed by Cozewith.[9] After the initial constant estimation, we verified those constants that exhibited higher sensitivity, considering the following experimental parameters: ethylene content, molecular weight, polydispersity, and polymer yield. Finally, the constants with more sensitivity were estimated by the least-mean-square method using the SPEEDUP software, and their standard mean deviations are also quoted in Table IV.

Comparing the kinetic constants, we observe that Podolnyi considered the activation constant as infinite, that is, an instantaneous reaction. On the other hand, Cozewith estimated it as 10^2 mol L^{-1} min^{-1} and he did not take into account the influence of Al/V ratio in the generation of the active species since his studies were performed in Al/V ratios higher than 5. Under such conditions, there is an equilibrium between formation and deactivation of active species, which means that no effect of the number of active species on the polymer characteristics is observed. The activation constant (k_a) estimated in our model is smaller probably due to the lower working temperature.

Cozewith, using a different vanadium-based catalyst system, was the only one that considered the influence of diene concentration in the catalyst deactivation. In our model, the diene deactivation constant (k_{x3}) was estimated from the polymer yield and ethylene conversion, under different diene concentrations.

Table III Simulation Parameters and Initial Conditions Used in the Theoretical Model

Parameters	Values	Initial Conditions	Values
P_{SET} (bar)	1.12	$C_1(0)$ (mol L^{-1})	2.3×10^{-4}
T_{SET} (°C)	15.0	Al_0/C_{10}	0.5 to 15.0
F_{ET} (L min^{-1})	1.23	$M_{ETL}(0)$ (mol L^{-1})	0.16
F_{PP} (L min^{-1})	1.36	$M_{PPL}(0)$ (mol L^{-1})	0.46
F_R (L min^{-1})	7.2	$M_{DI}(0)$ (mol L^{-1})	5.0×10^{-4} to 1.5×10^{-1}
$kla_{PP} = kla_{ET}$ (min^{-1})	0.4	$P_T(0)$ (bar)	1.10
U_G (cal min^{-1} °C^{-1} m^{-1})	271.72 ± 9.2	T (0) (°C)	0.0
$\overline{\Delta H_P}$ (cal mol^{-1})	1.0×10^4 ± 1.744.6	T_B (0) (°C)	−4.0
A_M (m^2)	0.1072	T_C (0) (°C)	−2.0
K_C (cal min^{-1} °C^{-1})	479.63 ± 25.0	y_{ET}/y_{PP} (0)	25/75
V_B (L)	4.5		
K_G (L min^{-1} $bar^{-0.5}$)	18.78		
V_C (L)	0.9		
$V_L = V_G$ (L)	1.0		

Table IV Kinetic Constants for Co- and Terpolymerization Models Proposed in the Literature and for this Model (L mol^{-1} min^{-1})

Reaction Step		Constant (mol L^{-1} min^{-1})	Cozewith[9] (37°C)[a]	Cozewith[7] (30°C)[b]	Podolnyi et al.[6] (20°C)[b]	Podolnyi et al.[6] (20°C)[a]	Present Model (15°C)[a]
Activation		k_a^*	1.66×10^2	1.66×10^2	$\propto$	$\propto$	$4.0 \times 10^1 \pm 1.0 \times 10^1$
Deactivation	Diene	k_{x3}	2.0×10^4	—	—	—	$2.0 \times 10^4 \pm 4.6 \times 10^3$
Chain	Ethylene	k_{y1}	8.3×10^1	8.33	2.0×10^1	2.0×10^1	8.33
initiation	propylene	k_{y2}	—	8.33	—	—	8.33
Chain	Ethylene	k_{11}	1.6×10^5	2.3×10^4	1.3×10^5	1.8×10^4	$2.5 \times 10^4 \pm 4.1 \times 10^3$
propagation		k_{12}	3.1×10^4	1.10×10^4	1.3×10^4	3.0×10^3	1.1×10^4
		k_{13}	3.8×10^4	—	—	2.6×10^5	9.3×10^4
	Propylene	k_{21}	3.8×10^4	1.42×10^4	1.1×10^4	7.2×10^4	$4.9 \times 10^4 \pm 4.2 \times 10^3$
		k_{22}	6.3×10^2	1.33×10^3	3.16×10^2	0	$8.0 \times 10^2 \pm 3.6 \times 10^1$
		k_{23}	0	—	—	2.5×10^5	—
	Diene	k_{31}	4.16×10^4	—	—	3.8×10^5	1.26×10^5
		k_{32}	0	—	—	5.3	—
Chain	Propylene	k_{trm2}	2.5×10^{-1}	1.33×10^{-1}	—	—	1.33×10^{-1}
transfer	Al-alquil	k_{tr2}^*	9.8×10^{-3}	—	—	—	9.8×10^{-3}
	Hydrogen	k_{tr1}	4.16×10^3	1.2×10^3	—	—	—
Chain	Cat deactivation	k_t^*	1.63×10^{-1}	3.5×10^{-2}	19	16	7.0×10^{-2}
termination	Diene	k_{tm3}	0	—	—	—	1.5
	Propylene	k_{tm2}	2.5×10^{-2}	1.466	0	—	7.0×10^{-1}

$k_x = 0$.
* Unit: min^{-1}
[a] Terpolymerization.
[b] Copolymerization.

In Table IV, we can also observe that all the authors agree that the initiation step takes place only with ethylene, excepting Cozewith,[9] who supposed that this step can start either with ethylene or propylene in equal probability. According to experimental data, we observe that the initiation step considering both monomers seems to be more suitable. If we considered the initiation step only with ethylene in the model, we would have an ethylene cumulative incorporation more heterogeneous than that observed experimentally.

All the authors agree that, in the case of copolymerization, the ethylene is the most reactive monomer and that the ethylene–ethylene addition constant (k_{11}) is the highest one. On the other hand, it is worth mentioning that Podolnyi, comparing co- and terpolymerization reactions, observed that the k_{11} and k_{12} constants were reduced in the presence of the third monomer. Similar results were obtained when we compared both reactions in the Cozewith and Podolnyi models, regarding the propylene–propylene addition constant (k_{22}), where its value is reduced or even neglected in the case of terpolymerization. Those considerations are based on the fact that the propylene homopolymerization under such temperatures (20–60°C) and with these catalytic systems is very unlikely.[9] Cozewith also observed that propylene–ethylene addition constant (k_{21}) is increased in the case of terpolymerization. In all those models, an increase in ethylene incorporation compared to propylene was verified when the third monomer was added. In our model, when we used the propagation constant proposed by Cozewith,[7] we observed lower ethylene incorporation than that determined experimentally. Thus, we fitted those constants in a more suitable way until achieving an ethylene incorporation similar to that observed experimentally.

With respect to diene addition, very different values are verified in the models in Table IV. The very high ethylene–diene (k_{13}) and diene–ethylene (k_{31}) propagation constants are compatible to experimentally observed yields in the case of high diene concentration. Concerning the diene–propylene (k_{32}) and propylene–diene (k_{23}) chain propagation constants, Podolnyi et al.[6] proposed very high values ($\cong 10^5$ mol L^{-1} min^{-1}), while Cozewith[7] neglected them due to their very low incorporation. In our study, the model can fit the experimental data, only when those constants were neglected.

According to those authors, the best transfer agent is hydrogen, followed by propylene, and finally by alkylaluminum. In our experimental system, we did not use hydrogen as a transfer agent. Thus, we could only estimate the influence of propylene (k_{trm2}) and alkylaluminum (k_{tr2}).

Concerning the termination chain, according to the models proposed in the literature, this step can occur by the influence of diene or propylene, or also by spontaneously catalyst deactivation. None of the authors in Table IV estimated the influence of diene on the termination step. As we worked with high diene concentrations, we included in our model the diene termination reaction. The kinetic constant was estimated from ethylene conversion data and polymer yields under different diene concentrations.

As we can see in Table IV, Podolnyi et al.,[6] even working at lower temperatures (20°C), presented higher kinetic constants when compared to those proposed by Cozewith for the same catalytic system. Comparing both Cozewith's models performed at different temperatures (30 and 37°C), we observe that the coherence of each kinetic constant at each different temperature is maintained, except for the propylene–propylene chain propagation, propylene chain termination, and catalyst deactivation constants. These differences may be attributed to the distinct catalytic systems employed. However, it seems that the comparison between co- and terpolymerization reaction constants is inadequate since the introduction of the third monomer causes considerable changes in the constant values.

RESULTS AND DISCUSSION

Before discussing the influence of *Al/V* ratios and of the diene concentration on EPDM terpolymerization, an example of the best fit in the case of instantaneous and cumulative ethylene incorporation in the polymer chain is worth illustrating.

According to Figure 2, the cumulative molar fraction of ethylene incorporated in the polymer, estimated by the model, has good agreement with those observed experimentally. We can also observe that the cumulative ethylene composition incorporated in the EPDM, for both experimental and theoretical cases, is kept constant along the reaction time. This cumulative homogeneity in composition is typical of systems that work under constant concentration of monomer. On the other hand, concerning the instantaneous ethylene incorporation predicted by the model, we can observe a decrease in ethylene incorporation for the first 3 min. Such results suggest a convective transfer control due to the high ethylene reactiv-

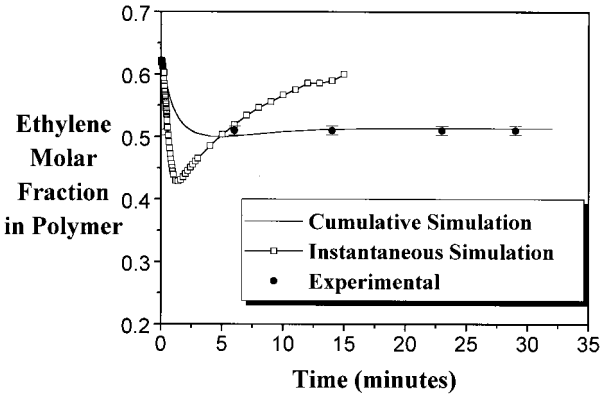

Figure 2 Experimental and simulation results of cumulative and instantaneous ethylene incorporation. *Al/V* = 8.3; [*V*] = 2.32×10^{-4} mol L^{-1}; [diene] = 1.8×10^{-3} mol L^{-1}.

ity, which causes an instantaneous lack of monomer and, consequently, a decrease in the ethylene incorporation. These results are also supported by other works in the literature[21] in which ethylene–propylene copolymerization was studied using a plug flow reactor (PFR) system. In this case, the variation of ethylene–propylene ratio in the gas phase due to the higher ethylene reactivity leads to a heterogeneous distribution.

After fitting the kinetic constants, we evaluated the effect of the initial *Al/V* ratio on activity and on polymer properties, keeping constant the diene concentration.

Initial *Al/V* Ratio Effects

Experimentally, the initial *Al/V* ratio was varied from 0.5 to 15.0, using a constant diene concentration (1.8×10^{-3} mol L^{-1}). From experimental results, it was observed that for *Al/V* ratios lower than 2, no reaction takes place since at least 2 alkylaluminum molecules to 1 of catalyst to form the active species is necessary.[10] For *Al/V* ratios between 2 and 8, we had previously observed that the yield increases until it reaches a plateau for ratio over 8,[22] probably due to an equilibrium between activation and deactivation of the catalytic species. In our proposed model, assuming that 100% of active species for *Al/V* corresponds to 8 and 0%, for *Al/V* = 2, we estimated the influence of alkylaluminum on the formation of the active species (k_a).

The influence of initial *Al/V* ratio in the ethylene polymer incorporation can be observed in Figure 3.

Experimentally, we observed that up to *Al/V* = 8, there is a decrease in ethylene incorporation; and for higher *Al/V* ratios, its content is practically constant. At very low *Al/V* ratios, we observe that the mathematical model did not fit well the experimental data, although the model has taken into account the influence of *Al/V* ratio on the active species formation step. The higher ethylene incorporation observed for lower *Al/V* cannot be exclusively a consequence of small amount of active species, which may reduce the propylene insertion, but also due to any change on the nature of active species.

Table V presents the polymer characteristics for the *Al/V* ratio between 2.5 and 15.0. According to the literature,[23] for ethylene–propylene incorporation ratio, between 40 to 50%, the glass transition temperature (T_g) does not change significantly, from −52 to −40°C. The T_g values presented in Table V are coherent with data proposed in the literature.[23] The increase in diene incorporation (shown as iodine number) causes an increase in T_g values and it may account for the small T_g differences observed for the same ethylene content.

According to Table V, an increase in *Al/V* ratio from 8.5 to 15.0 leads to a decrease in viscometer molecular weight. The same behavior could be observed in the simulation process, as shown in Figure 4. The decrease in molecular weight as *Al/V* ratio grows might be due to the increase in alkylaluminum transfer reaction. Cozewith[7] did not observe such behavior when he varied the *Al/V* ratio over 8, probably because he worked in a continuous system, where the alkylaluminum has been constantly request for the catalyst alkylation.

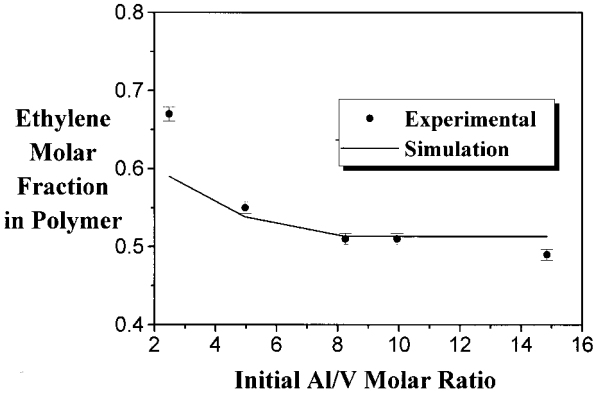

Figure 3 Experimental (●) and simulation (—) results of the effect of the initial *Al/V* molar ratio on the ethylene incorporation. [diene] = 1.8×10^{-3} mol L^{-1}; [*V*] = 2.32×10^{-4} mol L^{-1}.

Table V Polymer Characteristics Under Different Initial *Al/V* Molar Ratios[a]

Al/V Molar Ratio	Iodine Number	$\overline{M_V} \times 10^{-6}$ (uma)	T_g (°C)	Propylene Molar Fraction
2.5	20	1.00	−41	0.37
5.0	27	—	−41	0.45
8.3	25	0.86	−39	0.49
10.0	29	—	−44	0.49
15.0	28	0.54	−40	0.51

[a] $[V] = 2.32 \times 10^{-4}$ mol L^{-1}; [diene] $= 1.8 \times 10^{-3}$ mol L^{-1}

Diene Concentration Effects

The ENB concentration in the reactor was varied between 5.0×10^{-4} and 1.5×10^{-1} mol L^{-1}, keeping constant the *Al/V* ratio at 8.3. Experimentally, we can observe that the solution color changes from uncolored to violet after the diene addition, indicating the catalyst reduction from V(III) to V(II),[11] which is known to be inactive for Ziegler–Natta polymerization. Thus, the ENB acts on the active species formation step, and consequently on the polymerization yield, as we can see in Figure 5.

According to Figure 5, as we increase the diene concentration in the milieu, the reaction yield decreases. Experimentally, the reaction yield reduction starts at diene concentrations above 0.04 mol L^{-1}. The yield decreasing in the model seems to be governed by the higher deactivation and termination ratio promoted by the diene, when compared to the yield increase as a consequence of diene incorporation in the polymeric chain. The difficulty in estimating such behavior may be due to other parallel reactions, such as branching, gel formation, and diene-coupling reactions,[24] which were not considered in this model for simplification reasons. Recently, it was observed that such deactivation under high diene concentrations does not take place when metallocenes catalysts are employed.[25]

Table VI presents some properties of the polymers produced by different diene concentrations. Experimentally, we observe that as diene concentration increases, its incorporation in the polymer grows. The T_g is practically constant, excepting for very high diene concentrations, where T_g value becomes higher and the T_g curve profile less sharp. The increase in the diene incorporation leads to a larger number of branchings in the polymeric chain, reducing the free volume among the chains and, consequently, increasing the T_g. On the other hand, higher ethylene incorporation decrease the T_g values. Thus, as in our present case, both ethylene and diene incorporation increases along the data in Table VI; and as both parameter present antagonistic effect in T_g, it

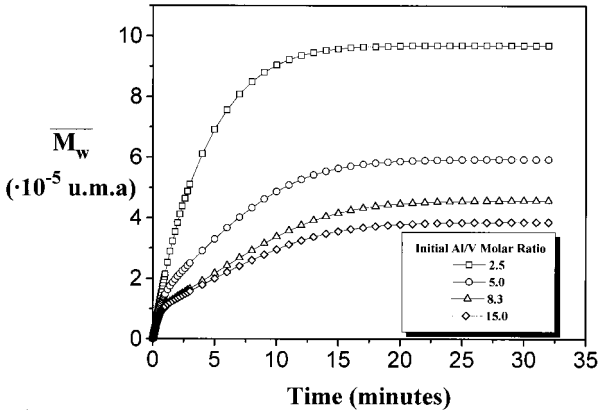

Figure 4 Effect of *Al/V* molar ratio on theoretical weight molecular weight. [diene] $= 1.8 \times 10^{-3}$ mol L^{-1}; $[V] = 2.32 \times 10^{-4}$ mol L^{-1}.

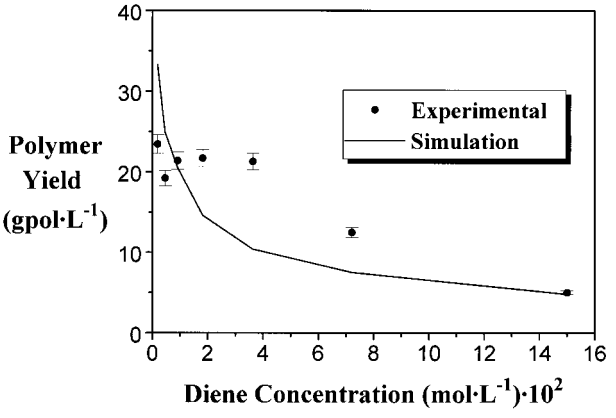

Figure 5 Experimental (●) and simulation (—) results of the effect of diene concentration on the polymer yield. *Al/V* = 8.3; $[V] = 2.32 \times 10^{-4}$ mol L^{-1}.

Table VI Polymer Characteristics Under Different Initial Diene Concentrations[a]

[diene] mol L^{-1}	$\overline{M_V}\ 10^{-5}$ (uma)	$\overline{M_W} \times 10^{-5}$ (GPC)	DP (GPC)	Iodine Number	T_g (°C)	Ethylene Molar Fraction
1.00×10^{-3}	7.2	—	—	17	−42	0.50
1.80×10^{-3}	8.6	5.0	3.8	25	−39	0.51
5.00×10^{-3}	5.7	—	—	25	−42	0.54
9.00×10^{-3}	1.2	3.0	30	33	−42	0.55
1.80×10^{-2}	cp[b]	cp[b]	cp[b]	45	−33	0.59

[a] $[V] = 2.32 \times 10^{-4}$ mol L^{-1}; $Al/V = 8.3$.
[b] cp = crosslinked polymer.

seems that this is the reason for the constancy in T_g data in this studied diene range.

Figure 6 shows the ethylene molar fraction in EPDM as function of ENB concentration. The ethylene incorporated content grows as the diene concentration increases. As already mentioned, high diene concentration reduces the number of active species, and during the competition for the insertion at the active species, the higher intrinsic reactivity of ethylene guarantees its higher incorporation. The model confirms this hypothesis and agrees with the experimental data, as we can see in Figure 6.

The diene concentration between 3.6×10^{-2} and 1.5×10^{-1} mol L^{-1} leads to gel formation, as a consequence of the higher number of the chain crosslinkings. Those polymers were insoluble and did not allow us to perform their characterization.

According to GPC determination, the polydispersity changes from 3.8 to 30.0 with the increase in diene concentration. The molecular weight determination with viscometer demonstrated also a reduction in molecular weight as diene concentration grows. The dynamic simulation of the weight-average molecular weight obtained under different diene concentration is shown in Figure 7.

If we used the constants initially proposed in Table II, we would observe the reduction in the yield, but we would not be able to verify the reduction in molecular weight as we experimentally determined. This correction was performed, considering the number of vanadium active species in the presence of high diene concentrations. According to the literature, for diene concentrations around 9.0×10^{-3} mol L^{-1}, only 20% of the initial catalyst concentration remains in an active form.[11] This reduction factor was used in the model. For even higher concentrations, a proportional factor was then employed. This reduction in catalyst concentration increases the number of alkylaluminum free species and, consequently, augments the transfer reactions, decreasing the molecular weight.

In our proposed model, for the first minutes of polymerization, we can observe in Figure 7 a higher molecular weight for higher diene concen-

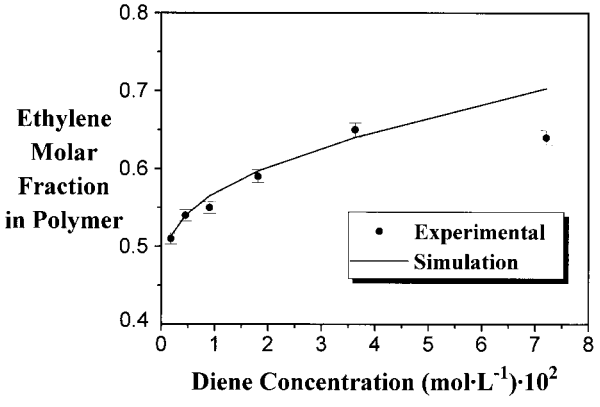

Figure 6 Experimental (●) and simulation (—) results of the effect of diene concentration on the ethylene incorporation. $Al/V = 8.3$; $[V] = 2.32 \times 10^{-4}$ mol L^{-1}.

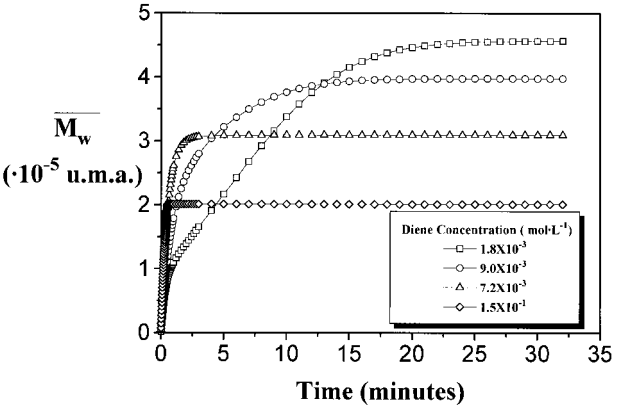

Figure 7 Effect of diene concentration on theoretical weight molecular weight. $Al/V = 8.3$; $[V] = 2.32 \times 10^{-4}$ mol L^{-1}.

trations. This can be attributed to the fact that initially we have a significant number of ethylene-ending chains, which lead to a higher diene incorporation and, consequently, to a higher molecular weight. This fact takes place since we assumed high ethylene–diene propagation constants. Cozewith, employing the vanadium salt–$AlEt_2Cl$ system, also observed the increase in polymer molecular weight with the diene concentration.[7] Nevertheless, he did not observe the same behavior for the first minutes of reaction because he worked with a CSTR system, with continuous feeding of catalyst, cocatalyst, and monomers. Then, at relative low diene concentration (1×10^{-4} mol L^{-1}), there is not a drastic catalyst reduction.

In our proposed model, the polydispersity does not grow with diene concentration, as we could observe experimentally. These results suggest that the model fails to fit experimental data for high diene concentrations since we neglected branching reactions promoted by the diene, which may become important for very high concentrations.

CONCLUSION

The present model fits reasonable well the experimental data for Al/V ratios up to 15, being in accord to many observations already described in the literature. The reaction needs at least 2 atoms of Al to generate the active species, which grows in activity until $Al/V = 8$, and then is kept constant. The ethylene incorporation in this range can also be simulated.

The diene concentration affects the number of active species since it leads to vanadium reduction, deactivating the catalytic species. The decrease in yield and in molecular weight can be simulated by this model. Nevertheless, it failed to reproduce the polydispersity observed experimentally since the branching reaction, which were neglected due to the low reactivity of the remaining double bond in ENB, cannot be excluded from the model for high diene concentrations.

Diene concentrations below 10^{-3} mol L^{-1} and Al/V ratio over 8 lead to small variations in polymer properties.

The proposed model was able to predict and to explain the influence of Al/V ratio and diene concentration on the polymer characteristics. For extreme conditions, the model failed, as already mentioned, due to the presence of other neglected reactions (such as branching), the products of which are very difficult to characterize.

This work was supported by PADCT-FINEP and FAPERGS. The authors thank Dr. Jorge Zacca for useful discussion.

NOMENCLATURE

A_M, A_{EXT}	internal and external area (m^2)
Al, Al_0	alkylaluminum concentration (mol L^{-1})
C_{10}, C_1, C_2	vanadium and active species concentration (mol L^{-1})
Cp_L Cp_R	heat capacity of liquid phase and cooling liquid (cal Kg^{-1} °C^{-1})
D	deactivated species concentration (mol L^{-1})
DP	polydispersity
F_{ET}, F_{PP}, F_G, F_R	volumetric flow of ethylene, propylene, gas phase, and cooling liquid (L min^{-1})
K_C	heat transfer constant (cal min^{-1} °C^{-1})
K_G	flow constant for the gas phase (L min^{-1} $bar^{-0.5}$)
kla_{ET}, kla_{PP}	mass transfer coefficient based on liquid phase for ethylene and propylene (min^{-1})
M_1, M_2, M_3	ethylene, propylene, and diene concentration (mol L^{-1})
M_{DI}	diene concentration (mol L^{-1})
M_{ETEQ}, M_{ETF}, M_{ETG}, M_{ETGS}, M_{ETL}	ethylene concentration at equilibrium, feed, gas phase, gas out, and liquid phase (mol L^{-1})
M_{PPEQ}, M_{PPF}, M_{PPG}, M_{PPGS}, M_{PPL}	propylene concentration at equilibrium, feed, gas phase, gas out, and liquid phase (mol L^{-1})
$\overline{M_N}$, $\overline{M_W}$	number- and weight-average molecular weight (uma)
P_1, P^0, P^1, P^2	activated ethylene units, zeroth, first- and second-order moments for live chains terminated with ethylene (mol L^{-1})
P_{ATM}, P_{SET}, P_T	atmospheric, set point, and reactor pressure (bar)

Q_1, Q^0, Q^1, Q^2	activated propylene units, zeroth, first-, and second-order moments for live chains terminated with propylene (mol L^{-1})
R_P	total propagation reaction rates (mol L^{-1})
R^0, R^1, R^2	zeroth, first-, and second-order moments for live chains terminated with diene (mol L^{-1})
r_{ET}, r_{PP}, r_{ENB}	ethylene, propylene, and diene reactivity on the polymeric chain
S^0, S^1, S^2	zeroth, first-, and second-order total moments (mol L^{-1})
S_{ET}, S_{PP}	ethylene and propylene solubility (mol L^{-1} bar^{-1})
T, T_B, T_C, T_{SET}	reactor, heat exchanger, jacket, and set temperature (°C)
U_G	overall heat transfer coefficient (cal min^{-1} $°C^{-1}$ m^{-2})
U^0, U^1, U^2	zeroth, first-, and second-order moments for all dead chains (mol L^{-1})
V_B, V_C, V_G, V_L,	heat exchanger, jacket, gas phase, and liquid phase volume (L)
w	weighted molecular weight of teorethical monomer (g mol^{-1})
x_{HX}	*n*-hexane molar fraction (mol mol^{-1})
xp_{ET}, xp_{PP}, xp_{ENB}	cumulative molar fraction of ethylene, propylene, and diene in the polymer (mol mol^{-1})
Y_p	polymer concentration on the reactional medium (g L^{-1})
y_{ET}, y_{PP}	ethylene and propylene mass fraction on gas phase
$\overline{\Delta H}_P$	heat of polymerization (cal mol^{-1})
ρ_R, ρ_G, ρ_L	cooler, gas, and liquid phase density (kg m^{-3})

REFERENCES

1. J. B. P. Soares and A. E. Hamielec, *Macromol. Theory Simul.,* **4,** 1085 (1995).
2. J. A. Debling, G. C. Han, F. Kuijpers, J. Verburg, J. Zacca, and W. H. Ray, *AlChE J.,* **40,** 506 (1994).
3. I. A. Jaber and W. H. Ray, *J. Appl. Polym. Sci.,* **49,** 1709 (1993).
4. C. M. Chen and W. H. Ray, *J. Appl. Polym. Sci.,* **49,** 1573 (1993).
5. A. Valvassori, G. Sartori, G. Mazzani, and G. Pajaro, *Makromol. Chem.,* **61,** 46 (1963).
6. Y. B. Podolnyi, G. Solovyeva, and Y. Komenev, *Polym. Sci. USSR,* **A16,** 3224 (1974).
7. C. Cozewith, *Proceedings of the 73rd AIChE Meeting,* Chicago, 1980.
8. V. N. Pronyayev, I. D. Afanasev, and G. A. Kovaleva, *Polym. Sci. USSR,* **27,** 1448 (1985).
9. C. Cozewith, *AIChE J.,* **34,** 272 (1988).
10. F. P. Baldwin and G. Ver Strate, *Rubber Chem. Technol.,* **45,** 709 (1972).
11. M. Dolatkhani, H. Cramail, and A. Deffieux, *Macromol. Chem. Phys.,* **197,** 289 (1996).
12. W. K. A. Shaffer and W. H. Ray, *J. Appl. Polym. Sci.,* **65,** 1053 (1997).
13. S. Floyd, R. A. Hutchinson, and W. H. Ray, *J. Appl. Polym. Sci.,* **32,** 5451 (1986).
14. J. C. Lamont and S. Scott, *AIChE J.,* **16,** 513 (1970).
15. P. H. Calderbank, *Trans. Inst. Chem. Eng.,* **36,** 443 (1958).
16. W. H. Ray, T. L. Douglas, and E. W. Godsalve, *Macromolecules,* **4,** 162 (1971).
17. R. Secchi, E. R. Lima, and J. C. Pinto, *Polym. Eng. Sci.,* **30,** 1209 (1990).
18. R. A. Hutchinson, C. M. Chen, and W. H. Ray, *J. Appl. Polym. Sci.,* **44,** 1389 (1992).
19. E. Wilhelm and R. Battino, *Chem. Rev.,* **73,** 1 (1973).
20. J. Villadsen and M. L. Michelsen, *Solution of Differential Equations by Polynomial Approximation,* Prentice-Hall, New York, 1978, p. 327.
21. C. Cozewith, G. Ver Strate, and S. Ju, *Macromolecules,* **21,** 3360 (1988).
22. M. C. Haag, J. H. Z. dos Santos, F. C. Stedile, M. A. de Araújo, J. Dupont, and I. J. R. Baumvol, *J. Appl. Polym. Sci.,* **68,** 535 (1998).
23. G. Ver Strate, *Encyclopedia of Polymer Science and Engineering,* Vol. 6, Wiley, New York, 1986, pp. 522–525.
24. G. Ver Strate, *Science and Technology of Rubber,* Academic Press, New York, 1978, p. 75.
25. A. Malmberg and B. Löfgren, *J. Appl. Polym. Sci.,* **66,** 35 (1997).